Eur Biophys J (2015) 44:131–138
DOI 10.1007/s00249-015-1008-y

ORIGINAL PAPER

EBSA
Biophysics in Europe

Novel biophysical determination of miRNAs related to prostate and head and neck cancers

Kristyna Hudcova · Libuse Trnkova · Iva Kejnovska · Michaela Vorlickova · Jaromir Gumulec · Rene Kizek · Michal Masarik

Received: 19 August 2014 / Revised: 15 December 2014 / Accepted: 13 January 2015 / Published online: 4 February 2015

Abstract In this study we have chosen a new approach and characterized three miRNAs (miR-23a, miR-34a and miR-320a) related to prostate cancer and head and neck cancer by spectral (circular dichroic and UV-absorption spectra) and electrochemical (voltammetry at graphite and mercury electrodes) methods. The spectral and voltammetric results, reflecting different nucleotide sequences of miRNAs, were complemented by the results of DNAs(U) having the same oligonucleotide sequences as miRNAs. The effect of the substitution of ribose for deoxyribose was shown and structural diversity was confirmed. The stability of RNA and DNA(U) was studied using CD and UV-absorption spectroscopy and melting points were calculated. MiRNA-320a with the highest content of guanine provided the highest melting point. With respect to the rapid progress of miRNA electrochemical sensors, our results will be useful for the research and development of sensitive, portable and time-efficient miRNA sensors, which will be able to diagnose cancer and other diseases.

Keywords miRNA · Circular dichroism · Electrochemistry · Prostate cancer · Head and neck cancer

K. Hudcova · J. Gumulec · M. Masarik (✉)
Department of Pathological Physiology, Faculty of Medicine, Masaryk University, Kamenice 5, 625 00 Brno, Czech Republic
e-mail: masarik@med.muni.cz

K. Hudcova · L. Trnkova · J. Gumulec · R. Kizek · M. Masarik
CEITEC, Brno University of Technology, Technicka 3058/10, 616 00 Brno, Czech Republic

L. Trnkova
Department of Chemistry, Faculty of Science, Masaryk University, Kamenice 5, 625 00 Brno, Czech Republic

I. Kejnovska · M. Vorlickova
Institute of Biophysics v.v.i., Academy of Sciences of the Czech Republic, Kralovopolska 135, 612 65 Brno, Czech Republic

I. Kejnovska · M. Vorlickova
CEITEC, Masaryk University, Kamenice 5, 625 00 Brno, Czech Republic

Introduction

MicroRNAs (miRNAs) are small, non-coding ribonucleic acids (ncRNAs) that regulate gene expression at the post-transcriptional level (Mirnezami et al. 2009). The biogenesis of miRNAs is a multilevel process involving many enzymes and proteins; hence, its regulation is quite different from the previously described regulators of gene expression. Within the canonical model of biogenesis, genes for miRNAs contain their own promoters and are transcribed by RNA polymerase II into primary transcripts (pri-miRNA) (Bartel 2007). The effect of miRNAs is most often based on binding to the untranslated region (3'UTR) of the target mRNA, which causes the degradation (or inhibition) of the target mRNA and can be seen in many cellular processes such as proliferation, differentiation, apoptosis, metastases, angiogenesis and the immune response (Mattie et al. 2006; Scapoli et al. 2010). Recently, many studies have shown that miR-23a, miR-34a and miR-320a are associated with prostate and head and neck cancer (HNC) (Ayaz et al. 2013; Hsieh et al. 2013; Kumar et al. 2012; Mattie et al. 2006; Scapoli et al. 2010; Yamamura et al. 2012). Prostate cancer (PCa) is the second most frequently diagnosed cancer and the second leading cause of cancer death in males in developed countries (Jemal et al. 2011). HNC, which includes head and neck squamous cell carcinoma—cancers of the oral cavity, larynx, oropharynx and hypopharynx, is

the sixth most common cancer malignancy in the world (Warnakulasuriya 2009). Important risk factors include frequent consumption of alcoholic beverages and tobacco (Zygogianni et al. 2011) and human papillomavirus infections (HPV) (Marur et al. 2010). As compared with the healthy subjects, the expression level of miR-23a is reduced in PCa, whereas in colorectal adenocarcinoma, the level is increased and miR-23a supports the migration and invasiveness of these tumor cells (Mattie et al. 2006). MiR-23a, with 12 other miRNAs, is significantly overexpressed in oral squamous cell carcinoma (Scapoli et al. 2010). In another study it was found that 1′-acetoxychavicol acetate (ACA) may have anticancer effects against human HNC through the downregulation of miR-23a, which can repress tumor suppressor PTEN (Wang et al. 2013). Recent studies have pointed to the role of miR-34a as a tumor suppressor in many types of cancer including PCa, gastric cancer, cervical cancer, hepatocellular carcinoma and HNC (Cao et al. 2014; Chakraborty et al. 2014; Kumar et al. 2012; Liang et al. 2013; Liu et al. 2011; Ribeiro and Sousa 2014; Yamamura et al. 2012; Yang et al. 2014). The enforced expression of miR-34a in bulk or purified CD44+ PCa cells inhibited clonogenic expansion, tumor regeneration and metastasis (Liu et al. 2011). MiR-34a regulates the levels of PCa protooncogene c-MYC, which activates genes stimulating proliferation and is frequently deregulated in tumors. MiR-34a also inhibits cell proliferation in vitro (cell line PC-3) and in vivo, and it promotes apoptosis in PCa (Yamamura et al. 2012). MiR-34a plays an important role in the p53 protein pathway, the position of which is unique for cancer malignancy in almost all types of tumors. P53 activates the expression of miR-34a and regulates a feedback loop when miR-34a inhibits SIRT1, resulting in acetylation and p53 activation (Liang et al. 2013). Significant downregulation of miR-34a was observed in HNC patients as well as in HNC cell lines (Kumar et al. 2012). The regulatory axis of p53/miR-34a has also proved to be very important in controlling Bax-dependent apoptosis in non-small-cell lung carcinoma cells (Chakraborty et al. 2014). Mir-320a regulates the expression of PFKm (phosphofructokinase), which is a glycolytic enzyme of muscle type involved in the regulation of glycolysis—and it is known that cancer cells have a modified metabolism and increased aerobic glycolysis, which is why this miRNA is so important for cancer research (Tang et al. 2012). In PCa, the expression of miR-320a is significantly reduced; miR-320a inhibits the expression of catenin by annealing to the 3 ‘UTR region of mRNA and suppresses the stem cell-like characteristics for PCa. This means that miR-320a is a key negative regulator in prostate tumor-initiating cells (Hsieh et al. 2013). In laryngeal squamous cell carcinoma, which is the second most common HNC worldwide, the significantly upregulated miR-320a may thus serve as a biomarker of this disease (Ayaz et al. 2013).

Typical strategies for studying miRNAs are northern blotting (NB), qRT-PCR, in situ hybridization (ISH) and microarrays technologies (Hamidi-Asl et al. 2013). These techniques are well known and described, including possibilities for their modifications, which may be using locked nucleic acids (LNAs) in NB (Varallyay et al. 2008), ISH (Obernosterer et al. 2007) or qRT-PCR (Raymond et al. 2005). Nanomaterial-based assays have become popular; their use is sensitive, specific and often label-based or requiring a hybridization step. Modifications of this technique can use electroanalytic tags (Gao and Yang 2006), magnetic bead-based bioassay (Bettazzi et al. 2013) or a bioassay based on the ruthenium oxide nanoparticle-initiated deposition of an insulating film (Peng and Gao 2011). There are already many techniques conductive to using electrochemistry to detect miRNA (de Planell-Saguer and Rodicio 2011; Hamidi-Asl et al. 2013) and also spectroscopy (Driskell and Tripp 2010). Deamination of cytosine to produce uracil is a common and potentially mutagenic lesion in the genomic DNA (Larson et al. 2008). Uracil in DNA results from the spontaneous or enzymatic deamination of cytosine, resulting in mutagenic U:G mispairs (Sousa et al. 2007).

In this study we used for the first time the linear sweep voltammetry and elimination voltammetric procedure in connection with the pencil graphite electrode and circular dichroism (CD) for the determination of the miRNA structures and their changes. For the comparison of DNA and RNA, we used the DNA backbone with the base of uracil in which the presence of mutagenic cells has been demonstrated.

Materials and methods

RNA isolation and reverse transcription

Total RNA was obtained from the sera of patients with PCa (at St. Anne’s University Hospital Brno). The study was conducted in line with the principles of the Declaration of Helsinki and was approved by the Ethics Committee of the Faculty of Medicine, Masaryk University Brno. In total, we used 38 serum samples from patients and 10 serum samples from healthy males. Isolation from the patients’ sera was performed by using the commercial High Pure miRNA isolation kit (Roche, Switzerland). According to manufacturer’s instructions, 10 ng of isolated miRNA was transcribed using the TaqMan® microRNA reverse transcription kit (Applied Biosystems, USA), and 1.33 µl of transcribed miRNA was used directly in the real-time PCR reaction.

Quantitative real-time polymerase chain reaction (qRT-PCR)

The qRT-PCR was performed in triplicate using the TaqMan gene expression assay system with the 7500 real-time PCR system (Applied Biosystems, USA). The primer and probe sets were selected from TaqMan miRNA expression assays: hsa-miRNA-23a (assay ID: 000399), hsa-miRNA-34a (assay ID: 000426) and hsa-miR-320a (assay ID: 002277). The qRT-PCR was performed under the following amplification conditions: total volume 20 µl, initial denaturation 95 °C/10 min, then 45 cycles 95 °C/15 s, 60 °C/1 min. The amplified DNA was analyzed using the CT (cycle threshold) values of cycle expression for each miRNA. SW Excel 2007 (Microsoft, USA) was used to arrange the data set. SW Statistica 9.1 (StatSoft, USA) was used to perform the statistical analysis and chart construction.

Biophysical analysis

MiRNAs synthetic oligonucleotides (hsa-miR-23a: AUCAC AUUGCCAGGGAUUUCC, hsa-miR-34a:UGGCAGUGU CUUAGCUGGUUGU and hsa-miR-320a:AAAAGCUGG GUUGAGAGGGCGA) were purchased from Sigma-Aldrich (MO, USA) and used for analysis by LSV or CV (linear sweep voltammetry or cyclic voltammetry), CD and UV-absorption measurements. Lyophilized oligonucleotides were dissolved in miliQ-H_2O to the milimolar concentration according to nucleosides. To compare the CD and UV-absorption spectra of the individual miRNAs, we used the same number and order of bases carried on DNA backbone as in miRNAs. The synthetic oligonucleotides of miRNAs with the DNA backbone (DNA(U)) were purchased from Sigma-Aldrich (MO, USA) as well and dissolved to an equal extent as miRNAs.

Linear sweep voltammetry (LSV) and cyclic voltammetry (CV)

Oxidation and reduction signals were recorded on the pencil graphite electrode (PeGE) and on the hanging mercury drop electrode (HMDE) in aqueous buffered solutions. Experimental conditions were as follows: the concentration of the oligonucleotides was 1×10^{-4} M; phosphate-acetate buffer (pH 4.55–7.47); room temperature (23 °C). The electrochemical analyzer AUTOLAB PGSTAT 20 (EcoChemie, Utrecht, The Netherlands) linked with the VA Stand 663 and controlled by the GPES Manager 4.9 software was connected to a set of three electrodes: PeGE (0.5 HB Tombow, Japan) with an effective area of 8.5 mm^2 or HMDE with an effective area of 0.4 mm^2 as a working electrode, Ag/AgCl/3 M KCl as a reference electrode and Pt wire as an auxiliary electrode. LSV or CV parameters corresponded to the scan rate: 100, 200, 400 mV/s; potential range: from 0 to −1.8 V (HMDE) and from 0 to 1.2 V (PeGE); accumulation time $t_a = 30$ s and $t_a = 0$ s for HMDE and PeGE, respectively; potential step: 2 mV. For a further data treatment, the potential-current values were exported to Excel. We also tried to analyze miRNAs on PeGE using square-wave voltammetry (SWV) and differential pulse voltammetry (DPV).

Elimination voltammetric procedure (EVP)

The essence of the elimination voltammetric procedure (EPV) (formerly known as elimination voltammetry with linear scan—EVLS) consists in the transformation of voltammetric currents into functions that are capable of eliminating some unwanted current components (e.g., diffusion, capacitive or kinetic). The transformation resulting in the elimination function is based on the different dependence of a current component on the scan rate (polarization speed). Elimination coefficients of the elimination function can be calculated by using the software developed by the authors of this article. There is a possibility to eliminate capacitive kinetic or diffusion currents as well as their combinations so we can eliminate selected current components concurrently. EVP improves voltammetric signals and not only increases the sensitivity of voltammetric methods, but also improves the separation of overlapping signals. Such signals can be, for example, overlapped reduction signals of adenine and cytosine on HMDE (Trnkova et al. 2003, 2006) or oxidation signals purine derivatives on graphite electrodes (Navratil et al. 2014). The form of the function eliminating the capacitive and kinetic current components and conserving the diffusion current component for scan rates of 200, 400 and 600 mV/s is as follows:

$$f(I) = -14.674 I_{200\ \mathrm{mV/s}} + 29.350 I_{400\ \mathrm{mV/s}} - 14.670 I_{600\ \mathrm{mV/s}}.$$

Circular dichroism (CD) and UV-absorption spectroscopy

CD and UV-absorption measurements were taken using the Jasco 815 dichrograph (Tokyo, Japan) in 0.1-cm path-length quartz Hellma cells placed in a thermostatic holder (23 °C). The concentration of miRNAs was 1×10^{-4} M (in nucleosides); phosphate-acetate buffer (pH 4.55–7.47). For CD spectra, the scan rate was 100 nm/min, averaging four measurements. CD signals are expressed as a difference $\Delta\varepsilon$ in molar absorption of the left- and right-handed circularly polarized light.

Results and discussion

To determine the function of biologically important molecules responsibly, it is necessary to investigate their structure

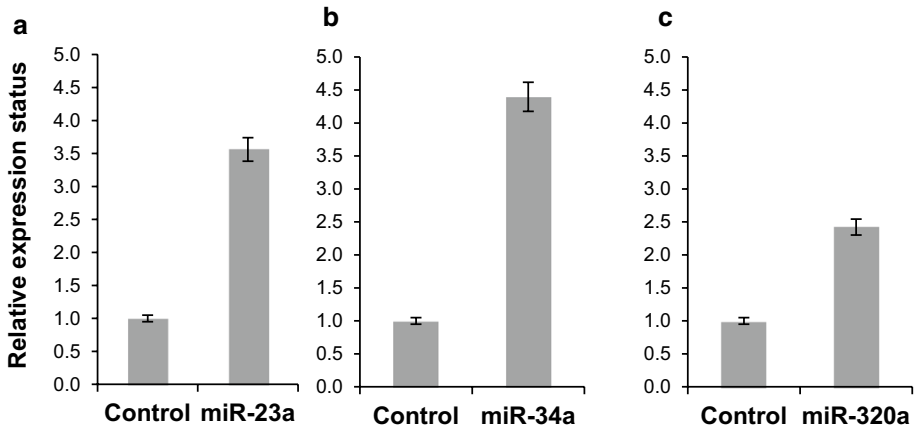

Fig. 1 Express status of miRNAs in patients' sera as compared with healthy controls. Comparison of the expression status of miRNAs (miR-23a, miR-320a and miR-34a) from the sera of patients with those of healthy controls using qRT-PCR. MiR-23a was expressed 3.5 times more in the patients' sera compared to the healthy controls (**a**); for miR-320a it was almost 2.5 times more (**c**). In the healthy controls, miR-34a was observed in a very small amount, while in the patients' sera, this miRNA showed good expression (**b**)

in dependence on eligible parameters, resulting in a correct understanding of the structure-function relationship. It could be an example of miRNAs, which have a very important regulatory function at the transcriptional level. We do not focus solely on the primary miRNA structures, but also on the secondary structures, whose influence on the behavior of RNA has a crucial role. De-coiled and more exposed structures of miRNA are more amenable to external effects such as mRNA annealing, creating complexes with proteins, hybridizing with the complementary structures and—for our purpose—annealing to the electrode surface. The secondary structure of miRNA was studied in the context of the primary transcript (pri-miRNA) and the precursor of miRNA (pre-miRNA) only (Diederichs and Haber 2006), but the description of the secondary structure of mature miRNA has never been studied by using the electrochemical and spectral methods such as voltammetry and CD spectroscopy. Compared to molecular-biological methods (qRT-PCR, NB, ISH), where the measurements are time-consuming, taking hours, voltammetry and CD spectroscopy are inexpensive, accessible and not time consuming (on an order of minutes).

Figure 1 shows the expression status of all three studied miRNAs—miR-23a, miR-34a and miR-320a—in the context of comparing healthy controls with PCa patients. The expression of the studied miRNAs in the patients with PCa is in larger quantities than in the healthy controls (by more than two times and in the following order: 34a > 23a > 320a); this is why we chose them for this study. From a biological point of view, these miRNAs are of interest to us and can be used as a suitable target for study using electrochemical and spectral methods. PCR methods inform about the primary structure level of miRNAs. To learn about their secondary structure, we need other approaches applying electro- and spectral analysis.

The direct oxidation of adenine and guanine in the nucleotide chains on bare carbon electrodes showed a poor response with a slow electron transfer, and the oxidation of adenine required a relatively higher overpotential than that of guanine. We investigated the guanine oxidation signals of miRNAs on PeGE by means of voltammetry in connection with our elimination procedure. A comparison of the oxidation peaks for all three miRNAs, measured by LSV using PeGE and evaluated by EPV is shown in Fig. 2a. Guanine peaks are situated around a potential of 1.1 V (vs. Ag/AgCl/3 M KCl). For the EPV analysis, three polarization rates (200, 400 and 600 mV/s) were used and a corresponding elimination function was calculated. The content of guanine in Fig. 2b corresponds with the peak height of each miRNA. In miR-320a with the highest content of guanine (45.5 % of the total), the highest peak was observed. The smallest peak was exhibited by miR-23a in which the content of four guanines was the lowest of all miRNAs.

To determine differences between the RNA and DNA skeletons, electrochemical (LSV analysis on HMDE) and spectroscopic (CD spectroscopy) analyses were carried out. Using electrochemistry (CV on a mercury electrode), we demonstrated that the RNA fragments form a single peak corresponding to the oxidative peak for guanine (Studnickova et al. 1989), while DNA(U) forms two peaks in the same region of potentials (Fig. 3a, b). The oxidation guanine signal (G peak) is known especially from the studies of oligodeoxynucleotides. It corresponds to the oxidation of the reduced product of guanine (7,8-dihydroguanine) proceeding at very negative potentials (more than −1.6 V) (Trnkova et al. 1980). The prerequisite for obtaining an oxidative signal is the accessibility of guanine residues of the oligonucleotide chain to the electrode surface. The dual oxidation guanine peak is a characteristic feature of

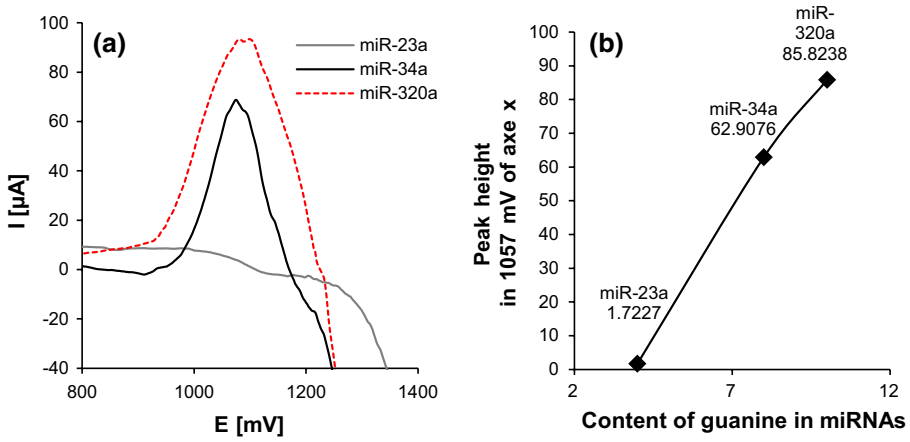

Fig. 2 Elimination voltammetric guanine peaks on the PeGE and dependence of these peak heights on the content of guanine. Comparison of guanine peaks (EPV from LSV as current-potential dependence) for three miRNAs (miR-23a, miR-34a, miR-320a) (1×10^{-4} M) peak (**a**) in phosphate–acetate buffer (pH 5.0), scan rate: 200,400,600 mV/s; activation of PeGE surface at potential −1.4 V (time 60 s); pre-treatment of PeGE by miRNA at potential 0 V (time 10 min). Peak height increases with the content of guanine in each miRNA (**b**)—measured under the same conditions as in (**a**)

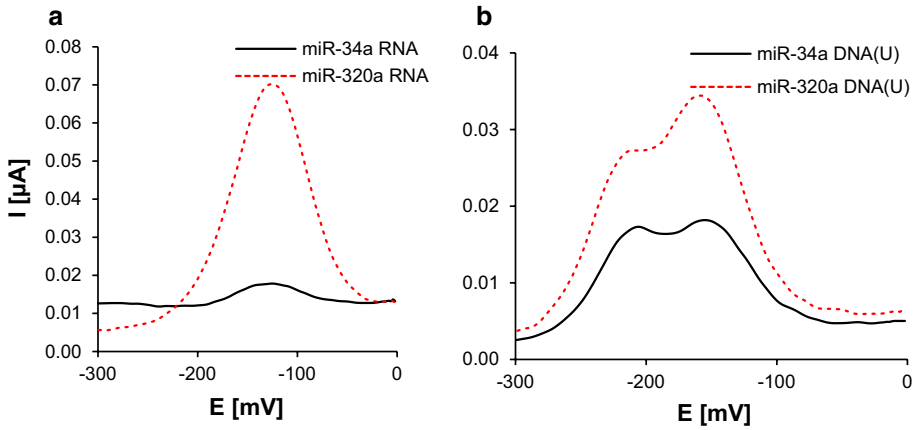

Fig. 3 Comparison of the guanine peak for RNA and DNA(U) backbone structures of two miRNAs using the mercury electrode. LSV as current-potential dependence for two forms of backbone structures—RNA and DNA(U) measured on miRNAs (1×10^{-4} M) in the phosphate-acetate buffer (pH 5.0), scan rate: 400 mV/s; accumulation potential −0.1 V and accumulation time 60 s. LSV curves were measured on a hanging mercury drop electrode. It is evident that the RNA structure of the sugar-phosphate backbone forms only one peak (**a**), while the DNA(U) structure forms two oxidative peaks for guanine (**b**)

DNA fragments. In the same buffer solutions, RNA is able to provide only one guanine oxidation peak. The difference can be attributed to the DNA structure conditioned by ribose and deoxyribose and to the different interaction of sugar with the nucleotide backbone.

To characterize miRNAs and DNA(U) structures and to obtain more information about their secondary structure, we also used CD and UV-absorption spectroscopy. This study focuses on a basic characteristic of miRNA, so we used higher concentrations of synthetic oligonucleotides (10^{-4} M) than the relevant concentration of miRNA in biological samples (10^{-8} M). The signals obtained from the CD spectra shown in Fig. 4a, b, c indicate clearly that the CD spectra reflect significant differences in the secondary structures of the miRNAs. The CD spectrum for miR-23a (Fig. 4a) shows a huge positive peak at 270 nm, a shallow negative peak at 240 nm and specifically the presence of a negative peak at 210 nm, which are characteristic signs for the A-form arrangement of the RNA. The DNA fragment of the same sequence yields a CD spectrum with small amplitudes corresponding to that of a sequentially heterogeneous non-perfectly ordered B-DNA form. The MiR-34a spectrum (Fig. 4b) has a positive shoulder around 240–250 nm (at the places where the classical A-form has

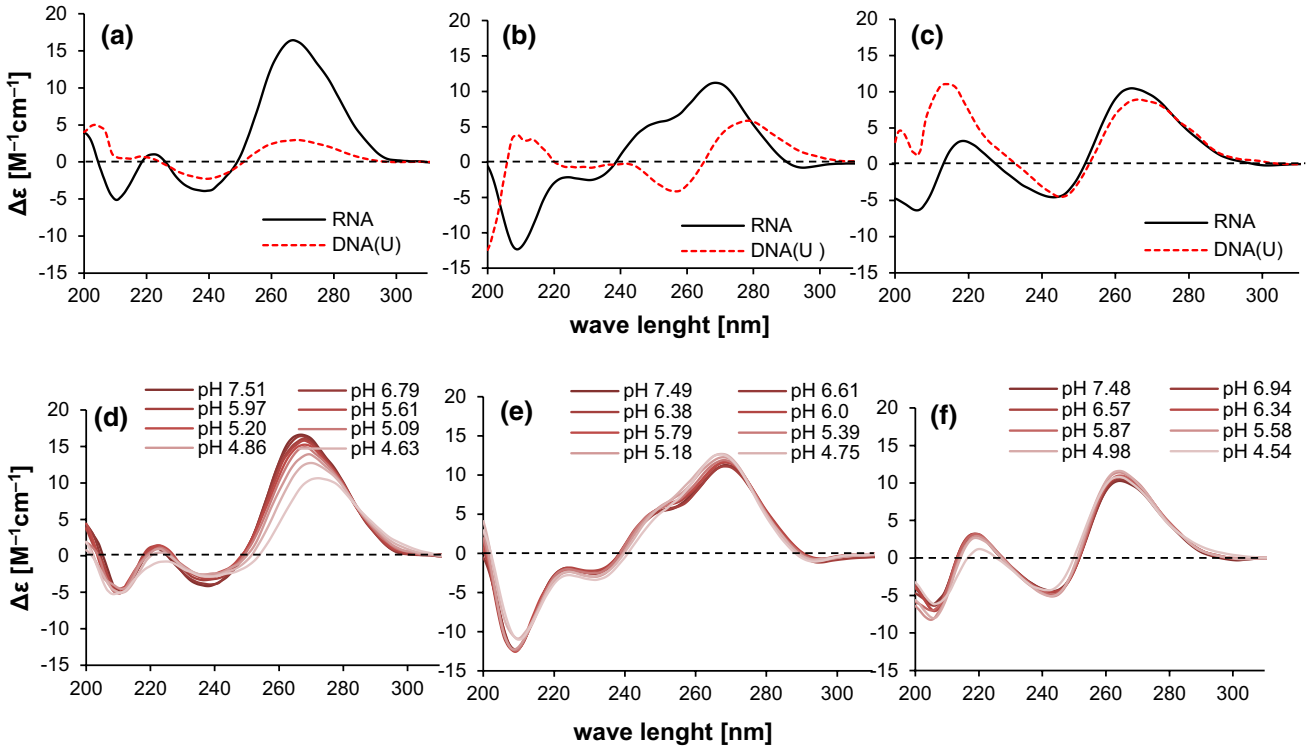

Fig. 4 CD spectra of miRNA and DNA-U. *Upper figures* CD spectra of miRNAs (**a** miR-23a, **b** miR-34a, **c** miR-320a—*black lines*) and DNA(U) (*red lines*) in phosphate–acetate buffer (pH 5.0). *Bottom figures* CD spectra of miRNAs (**d** miR-23a, **e** miR-34a, **f** miR-320a)—dependence on pH (the phosphate-acetate buffer). The concentration of miRNAs was 1×10^{-4} M

a shallow and rather negative minimum), which may result from the presence of non-standard pairing, such as G·U. The CD spectrum of the DNA analog corresponds to the standard B-form; only the positive CD peak is somewhat higher, and the whole spectrum is slightly shifted to longer wavelengths probably also because of the presence of the atypical U-base in the DNA structure. The CD spectrum of miR-320a (Fig. 4c) corresponds to the A-form RNA. Interestingly, its DNA analog provides nearly the same spectrum; only the minimum at 210 nm does not acquire negative values. The A-like spectrum of DNA could be a consequence of the probable A·U pairing enabled by the sequence. CD spectra of miRNAs do not distinctly change with changes of pH values (Fig. 4d, e, f) within a range of pH 7.5–4.5, where the A-form remains stable.

In this work, the stability of miRNA and DNA(U) structures was examined and quantified using UV absorption temperature dependences from which melting points (T_m°) were determined for both miRNA and DNA(U) (Table 1). The big difference in melting points ΔT_m° (14.5 °C) between RNA and DNA(U) for miR-34a might be due to the generation of several hairpin secondary structures according to its primary structure. In comparison, for miR-320a the difference in ΔT_m° is only 3 °C (and indicates significantly higher stability of the secondary structure related to more hydrogen bonds in this molecule of miRNA). Differences between RNA and DNA with uracil are evident; however, it can be generally concluded that miRNA has a lower melting point than the corresponding DNA(U).

Table 1 Comparison of melting points between RNA and DNA(U) forms of miRNA oligonucleotides

Melting points measured by UV-*absorption*	
RNA backbone of miRNA	
miR-23a	25.7 °C
miR-34a	32.0 °C
miR-320a	49.5 °C
DNA backbone of DNA(U)	
miR-23a	33.3 °C
miR-34a	46.5 °C
miR-320a	52.5 °C

Conclusions

Detection of miRNAs using electrochemical and spectral methods has become popular and useful. However, this still does not make possible the perfect characterization

of an ideal biomarker, which requires specificity, sensitivity, a low price, simplicity and reproducibility. This work attempts a combination of several techniques in the context of miRNA research that has not been used yet. PCR methodology focuses on a study with the help of the primary structure, which is the most common way to study miRNAs. As it is known that changes in the secondary structure are common in RNA, we decided to take advantage of this knowledge and to expand upon the subject. The difference between the DNA and RNA backbones has been demonstrated by LSV and CD. Different methods have been developed for the analysis of miRNA so far, but the combination of LSV, CD and UV-absorption methods using the information about the secondary structure for the characterization of miRNA has not been published yet. We expect that our novel approach will contribute to the development of a new label-free detection system for miRNA.

Acknowledgments This research was supported by the Central European Institute of Technology (CEITEC), Project CZ.1.05/1.1.00/02.0068, by the projects MUNI/A/1003/2013 and KONTAKT II (LH13053) of the Ministry of Education of the Czech Republic and IGA MZ NT14337-3/2013.

Conflict of interest The authors declare they have no competing interests as defined by the European Biophysics Journal or other interests that might be perceived to influence the results and discussion reported in this paper.

References

Ayaz L, Gorur A, Yaroglu HY, Ozcan C, Tamer L (2013) Differential expression of microRNAs in plasma of patients with laryngeal squamous cell carcinoma: potential early-detection markers for laryngeal squamous cell carcinoma. J Cancer Res Clin Oncol 139:1499–1506

Bartel DP (2007) MicroRNAs: genomics, biogenesis, mechanism, and function (reprinted from Cell, vol 116, pg 281–297, 2004). Cell 131:11–29

Bettazzi F, Hamid-Asl E, Esposito CL, Quintavalle C, Formisano N, Laschi S, Catuogno S, Iaboni M, Marrazza G, Mascini M, Cerchia L, De Franciscis V, Condorelli G, Palchetti I (2013) Electrochemical detection of miRNA-222 by use of a magnetic bead-based bioassay. Anal Bioanal Chem 405:1025–1034

Cao WG, Yang WP, Fan R, Li H, Jiang JS, Geng M, Jin YN, Wu YL (2014) miR-34a regulates cisplatin-induce gastric cancer cell death by modulating PI3K/AKT/survivin pathway. Tumor Biol 35:1287–1295

Chakraborty S, Mazumdar M, Mukherjee S, Bhattacharjee P, Adhikary A, Manna A, Khan P, Sen A, Das T (2014) Restoration of p53/miR-34a regulatory axis decreases survival advantage and ensures Bax-dependent apoptosis of non-small cell lung carcinoma cells. FEBS Lett 588:549–559

de Planell-Saguer M, Rodicio MC (2011) Analytical aspects of microRNA in diagnostics: a review. Anal Chim Acta 699:134–152

Diederichs S, Haber DA (2006) Sequence variations of microRNAs in human cancer: alterations in predicted secondary structure do not affect processing. Cancer Res 66:6097–6104

Driskell JD, Tripp RA (2010) Label-free SERS detection of microRNA based on affinity for an unmodified silver nanorod array substrate. Chem Commun 46:3298–3300

Gao ZQ, Yang ZC (2006) Detection of microRNAs using electrocatalytic nanoparticle tags. Anal Chem 78:1470–1477

Hamidi-Asl E, Palchetti I, Hasheminejad E, Mascini M (2013) A review on the electrochemical biosensors for determination of microRNAs. Talanta 115:74–83

Hsieh IS, Chang KC, Tsai YT, Ke JY, Lu PJ, Lee KH, Yeh SD, Hong TM, Chen YL (2013) MicroRNA-320 suppresses the stem cell-like characteristics of prostate cancer cells by downregulating the Wnt/beta-catenin signaling pathway. Carcinogenesis 34:530–538

Jemal A, Bray F, Center MM, Ferlay J, Ward E, Forman D (2011) Global cancer statistics. CA Cancer J Clin 61:69–90

Kumar B, Yadav A, Lang J, Teknos TN, Kumar P (2012) Dysregulation of microRNA-34a expression in head and neck squamous cell carcinoma promotes tumor growth and tumor angiogenesis. Plos One 7:1–13

Larson ED, Bednarski DW, Maizels N (2008) High-fidelity correction of genomic uracil by human mismatch repair activities. BMC Mol Biol 9:13

Liang YJ, Liu J, Feng ZH (2013) The regulation of cellular metabolism by tumor suppressor p53. Cell Biosci 3:1–10

Liu C, Kelnar K, Liu BG, Chen X, Calhoun-Davis T, Li HW, Patrawala L, Yan H, Jeter C, Honorio S, Wiggins JF, Bader AG, Fagin R, Brown D, Tang DAG (2011) The microRNA miR-34a inhibits prostate cancer stem cells and metastasis by directly repressing CD44. Nat Med 17:211–215

Marur S, D'Souza G, Westra WH, Forastiere AA (2010) HPV-associated head and neck cancer: a virus-related cancer epidemic. Lancet Oncol 11:781–789

Mattie MD, Benz CC, Bowers J, Sensinger K, Wong L, Scott GK, Fedele V, Ginzinger D, Getts R, Haqq C (2006) Optimized high-throughput microRNA expression profiling provides novel biomarker assessment of clinical prostate and breast cancer biopsies. Mol Cancer 5:1–14

Mirnezami AHF, Pickard K, Zhang L, Primrose JN, Packham G (2009) MicroRNAs: key players in carcinogenesis and novel therapeutic targets. Ejso 35:339–347

Navratil R, Jelen F, Kayran YU, Trnkova L (2014) A pencil graphite electrode in situ modified by monovalent copper: a promising tool for the determination of methylxanthines. Electroanalysis 26:952–961

Obernosterer G, Martinez J, Alenius M (2007) Locked nucleic acid-based in situ detection of microRNAs in mouse tissue sections. Nat Protoc 2:1508–1514

Peng YF, Gao ZQ (2011) Amplified detection of microRNA based on ruthenium oxide nanoparticle-initiated deposition of an insulating film. Anal Chem 83:820–827

Raymond CK, Roberts BS, Garrett-Engele P, Lim LP, Johnson JM (2005) Simple, quantitative primer-extension PCR assay for direct monitoring of microRNAs and short-interfering RNAs. Rna Publ Rna Soc 11:1737–1744

Ribeiro J, Sousa H (2014) MicroRNAs as biomarkers of cervical cancer development: a literature review on miR-125b and miR-34a. Mol Biol Rep 41:1525–1531

Scapoli L, Palmieri A, Lo ML, Pezzetti F, Rubini C, Girardi A, Farinella F, Mazzotta M, Carinci F (2010) MicroRNA expression profiling of oral carcinoma identifies new markers of tumor progression. Int J Immunopathol Pharmacol 23:1229–1234

Sousa MML, Krokan HE, Slupphaug G (2007) DNA-uracil and human pathology. Mol Asp Med 28:276–306

Studnickova M, Trnkova L, Zetek J, Glatz Z (1989) Reduction of guanosine at a mercury-electrode. Bioelectrochem Bioenerg 21:83–86

Tang HB, Lee M, Sharpe O, Salamone L, Noonan EJ, Hoang CD, Levine S, Robinson WH, Shrager JB (2012) Oxidative stress-responsive microRNA-320 regulates glycolysis in diverse biological systems. Faseb J 26:4710–4721

Trnkova L, Studnickova M, Palecek E (1980) Electrochemical-behavior of guanine and its derivatives. 1. Fast cyclic voltammetry of guanosine and calf thymus DNA. Bioelectrochem Bioenerg 7:643–658

Trnkova L, Jelen F, Postbieglova I (2003) Application of elimination voltammetry to the resolution of adenine and cytosine signals in oligonucleotides. I. Homooligodeoxynucleotides dA(9) and dC(9). Electroanalysis 15:1529–1535

Trnkova L, Jelen F, Postbieglova I (2006) Application of elimination voltammetry to the resolution of adenine and cytosine signals in oligonucleotides II. Hetero-oligodeoxynucleotides with different sequences of adenine and cytosine nucleotides. Electroanalysis 18:662–669

Varallyay E, Burgyan J, Havelda Z (2008) MicroRNA detection by northern blotting using locked nucleic acid probes. Nat Protoc 3:190–196

Wang HB, Shen L, Li XM, Sun ML (2013) MicroRNAs contribute to the anticancer effect of 1′-acetoxychavicol acetate in human head and neck squamous cell carcinoma cell line HN4. Biosci Biotechnol Biochem 77:2348–2355

Warnakulasuriya S (2009) Global epidemiology of oral and oropharyngeal cancer. Oral Oncol 45:309–316

Yamamura S, Saini S, Majid S, Hirata H, Ueno K, Deng G, Dahiya R (2012) MicroRNA-34a modulates c-Myc transcriptional complexes to suppress malignancy in human prostate cancer Cells. Plos One 7:1–12

Yang F, Li QJ, Gong ZB, Zhou L, You N, Wang S, Li XL, Li JJ, An JZ, Wang DS, He Y, Dou KF (2014) MicroRNA-34a targets Bcl-2 and sensitizes human hepatocellular carcinoma cells to sorafenib treatment. Technol Cancer Res Treat 13:77–86

Zygogianni AG, Kyrgias G, Karakitsos P, Psyrri A, Kouvaris J, Kelekis N, Kouloulias V (2011) Oral squamous cell cancer: early detection and the role of alcohol and smoking. Head Neck Oncol 3(2):1–12